



## Diaryl-substituted thiosemicarbazone: A potent scaffold for the development of New Delhi metallo- $\beta$ -lactamase-1 inhibitors

Jia-Qi Li<sup>a</sup>, Le-Yun Sun<sup>a</sup>, Zhihui Jiang<sup>b</sup>, Cheng Chen<sup>a</sup>, Han Gao<sup>a</sup>, Jia-Zhu Chigan<sup>a</sup>, Huan-Huan Ding<sup>a</sup>, Ke-Wu Yang<sup>a,\*</sup>

<sup>a</sup> Key Laboratory of Synthetic and Natural Functional Molecule of the Ministry of Education, College of Chemistry and Materials Science, Northwest University, Xi'an 710127, PR China

<sup>b</sup> Department of Pharmacy, General Hospital of Southern Theatre Command of PLA, Guangzhou 510010, PR China

### ARTICLE INFO

#### Keywords:

Antibiotic resistance  
Thiosemicarbazone  
Inhibitor  
Metallo- $\beta$ -lactamases  
NDM-1

### ABSTRACT

The superbug infection caused by New Delhi metallo- $\beta$ -lactamase (NDM-1) has become an emerging public health threat. Inhibition of NDM-1 has proven challenging due to its shuttling between pathogenic bacteria. A potent scaffold, diaryl-substituted thiosemicarbazone, was constructed and assayed with metallo- $\beta$ -lactamases (M $\beta$ LS). The obtained twenty-six molecules specifically inhibited NDM-1 with IC<sub>50</sub> 0.038–34.7  $\mu$ M range (except **1e**, **2e**, and **3d**), and **1c** is the most potent inhibitor (IC<sub>50</sub> = 0.038  $\mu$ M). The structure-activity relationship of synthetic thiosemicarbazones revealed that the diaryl-substitutes, specifically 2-pyridine and 2-hydroxybenzene improved inhibitory activities of the inhibitors. The thiosemicarbazones exhibited synergistic antimycobacterial actions against *E. coli*-NDM-1, resulted a 2–512-fold reduction in MIC of meropenem, while **1c** restored 16–256-, 16-, and 2-fold activity of the antibiotic on clinical isolates ECs, *K. pneumonia* and *P. aeruginosa* harboring NDM-1, respectively. Also, mice experiments showed that **1c** had a synergistic antibacterial ability with meropenem, reduced the bacterial load clinical isolate EC08 in the spleen and liver. This work provided a highly promising scaffold for the development of NDM-1 inhibitors.

### 1. Introduction

$\beta$ -Lactam antibiotics, as the most important and frequently used antimicrobial agents, constituting more than 50% of the antibiotics prescribed worldwide [1]. However, the overuse of antibiotics has exacerbated the emergence of bacterial resistance and caused a serious public health threat [2]. Bacteria resist antibiotics in many ways, and the most important way is the production of  $\beta$ -lactamases, which catalyze the cleavage of  $\beta$ -lactam rings of the antibiotics [3].  $\beta$ -Lactamases have been divided into A-D categories according to the amino acid homologous sequences [4]. Class A, C and D enzymes are called serine- $\beta$ -lactamases (S $\beta$ LS), which use a catalytic mechanism where an active site serine nucleophilically attacks the  $\beta$ -lactam carbonyl [5]. Class B enzymes, also called metallo- $\beta$ -lactamase (M $\beta$ L), are divided into B1, B2 and B3 subclasses according to amino acid sequence and Zn(II) content [6].

To combat antibiotic resistance, an ideal strategy is to develop  $\beta$ -lactamase inhibitors. Currently, the S $\beta$ LS inhibitors have been used in

clinic, such as clavulanic acid, tazobactam, avibactam, and sulbactam [7,8]. So far, many M $\beta$ LS inhibitors have been reported, such as  $\beta$ -lactam analogues [9], thiols [10–12], carboxylic acids [13,14], ebselen [15,16], rhodanines [17–19], and cyclic boronates [20–22]. However, there is no M $\beta$ L inhibitor for clinic purposes to date.

New Delhi metallo- $\beta$ -lactamase-1 (NDM-1), a B1 subclasses M $\beta$ L, hydrolyzes almost all  $\beta$ -lactam antibiotics, even meropenem or imipenem [23]. NDM-1 is plasmid-encoded, which facilitates its rapid transmission and makes inhibiting it a daunting challenge [24]. The clinical pathogenic bacteria with NDM-1, such as Carbapenem-Resistant Enterobacteriaceae (CRE), *K. pneumonia*, and *P. aeruginosa*, are serious resistant. Effective inhibitors of NDM-1 have been sought after extensively. Recently, some inhibitors of NDM-1 have been reported [25–28], including fungal natural product aspergillomarasmine A (AMA) [26], which restores the antibacterial activity of meropenem against *K. pneumoniae* expressing NDM-1, 1,4,7-triazacyclononane-1,4,7-triacetic acid (NOTA) and 1,4,7,10-tetraazacyclododecane-1,4,7,10-tetraacetic acid (DOTA), which exhibits synergistic antibacterial ability

\* Corresponding author.

E-mail address: [kwyang@nwu.edu.cn](mailto:kwyang@nwu.edu.cn) (K.-W. Yang).

<https://doi.org/10.1016/j.bioorg.2020.104576>

Received 30 September 2020; Received in revised form 16 December 2020; Accepted 16 December 2020

Available online 22 December 2020

0045-2068/© 2020 Elsevier Inc. All rights reserved.

with meropenem on the bacteria harboring NDM-1 [27]. Besides, piroindoline-thiadiazole (SIT-Z5) has been reported to be an effective inhibitor of NDM-1 [28].

The thiosemicarbazones have been reported to have a wide pharmacological activity, including antibacterial, antiviral, antiparasitic, antifungal, antimalarial, and anticancer [29–33]. Recently, several thiosemicarbazones have been used for clinical trials to treat cancer (see Fig. 1). 3-aminopyridinecarboxaldehyde thiosemicarbazone (3-AP, Phase II) irreversibly inhibits ribonucleotide reductase through metal chelating. [34,35]. Also, di-2-pyridylketone 4-cyclohexyl-4-methyl-3-thiosemicarbazone (DpC, Phase I) and (E)-N'-(6,7-dihydroquinolin-8(5H)-ylidene)-4-(pyridin-2-yl)piperazine-1-carbothiohydrazide (COTI-2, Phase I) have been used for the treatment of resistant cancers and gynecological malignant tumors [36]. Furthermore, the thiosemicarbazone has been reported to inhibit urease and tyrosinase by metal complexation [37]. The binding of the thiosemicarbazone to metal enlightened us that it may be used for the development of the M $\beta$ L inhibitors. Our goal is to develop the M $\beta$ L inhibitors with a new backbone and fight resistant bacterial infections by  $\beta$ -lactam antibiotics combined with these compounds (see Fig. 2).

In this work, twenty-six thiosemicarbazones (Fig. 2) were designed, synthesized, and characterized by  $^1\text{H}$  and  $^{13}\text{C}$  NMR (see supporting information) and confirmed by HRMS. The inhibitory activities of these compounds were evaluated with five M $\beta$ LS NDM-1, VIM-2, IMP-1, ImiS, L1. The inhibitory mode was investigated by thermodynamics, enzymatic kinetics, and inductively coupled mass spectrometry assays [26]. Also, the synergistic antibacterial activity of these thiosemicarbazones and meropenem against antibiotic-resistant strains were evaluated. Moreover, the antibacterial activity of **1c** combined with meropenem was also studied *in vivo*.

## 2. Results and discussion

### 2.1. Synthesis of thiosemicarbazones

Primary amines reacted with  $\text{CS}_2$  under basic condition overnight, iodine was added and stirred for 30 min to give thiocyanates. In isopropanol, thiocyanates further reacted with hydrazine hydrate to form thiosemicarbazides, which reacted with aldehydes at  $100^\circ\text{C}$  for 2 h to offer the final products thiosemicarbazones **1a-1k**, **2a-2h**, and **3a-3g**. The primary amines chosen have aromatics and aliphatics, including ethylamine, cyclohexylamine, *N*-butylamine, isobutylamine, aniline, *o*-toluidine, *p*-toluidine, 4-butylbenzylamine, 4-chlorobenzylamine, 4-methoxybenzylamine, and 2-ethylbenzylamine.

### 2.2. Activity evaluation

To investigate whether the synthetic thiosemicarbazones were the inhibitors of M $\beta$ LS, the activity evaluation was conducted on an Agilent UV8453 spectrometer using meropenem ( $40\ \mu\text{M}$ , monitoring at  $300\ \text{nm}$ ) as substrate. The thiosemicarbazones tested concentrations ranged from 0 to  $80\ \mu\text{M}$ .

Percent inhibition of thiosemicarbazones on M $\beta$ LS NDM-1, VIM-2, IMP-1, ImiS, and L1 using meropenem ( $40\ \mu\text{M}$ ) as substrate. Fig. 3 showed that the 2-pyridine substituted thiosemicarbazones exhibited

more than 63% inhibitory activities against NDM-1, but less than 35% on the other M $\beta$ LS. Therefore, NDM-1 was focused on inhibition studies for the remainder of this work.

The inhibitor concentrations causing 50% decrease of enzyme activity ( $\text{IC}_{50}$ ) of thiosemicarbazones **1a-1k**, **2a-2h**, and **3a-3g** against NDM-1 were determined. The substrate (meropenem) concentration is  $40\ \mu\text{M}$ . The  $\text{IC}_{50}$  data (Table 1) indicated that most thiosemicarbazones (except **1e**, **2e**, **3d**, **3f**, **3g**) had strong inhibitory efficacy against NDM-1, exhibiting an  $\text{IC}_{50}$  value in the  $0.038\text{--}25.7\ \mu\text{M}$  range, and **1c** was the most effective inhibitor ( $\text{IC}_{50} = 0.038\ \mu\text{M}$ ). Interesting is that the 2-pyridine and 2-hydroxyphenyl substituted derivatives had an  $\text{IC}_{50}$  in the range of  $0.038\text{--}5.48$  and  $0.12\text{--}13.4\ \mu\text{M}$ , respectively, which is smaller than the  $\text{IC}_{50}$  of the 4-hydroxyphenyl substituted compounds ( $15.4\text{--}34.7\ \mu\text{M}$ ), suggesting that the N and OH at ortho-position of benzene ring bound to Zn(II) at enzymatic active sites. A structure-activity relationship (SAR) was revealed through analysis the  $\text{IC}_{50}$  data, which is that the  $\text{R}_1$  substitutes 2-pyridine and 2-hydroxybenzene significantly improved the inhibitory activities of thiosemicarbazones against NDM-1 as compared to the same substitutes at 4-position, and the aromatic  $\text{R}_2$  substitutes make the inhibitors have better activities than the aliphatic substitutes.

Due to the best inhibitory potency of thiosemicarbazone **1c**, we assayed the time- and concentration-dependent inhibitions of it. Fig. 4 showed that the residual activity of NDM-1 decreased with the extension of the compound incubation with NDM-1, and the thiosemicarbazone showed the maximum inhibition after incubating with NDM-1 for about 30 min (Fig. 4a). Also, as increasing the thiosemicarbazone concentrations ( $6.25\text{--}500\ \text{nM}$ ), the residual activity of NDM-1 decreased, indicating that **1c** is a time- and concentration-dependent inhibitor of NDM-1. The time-course of inactivation of NDM-1 by EDTA with a concentration in the range of  $0.63\text{--}10\ \mu\text{M}$  was assayed. As shown in Fig. 4c, the inhibition model of EDTA against NDM-1 is similar to that observed with **1c** (Fig. 4b). Also, the inhibition curves of NDM-1 by **1c** in the presence of Zn (II) ions ( $1.0\ \mu\text{M}$ ) were assayed. The concentrations of **1c** ranged from  $6.25$  to  $500\ \text{nM}$ . As shown in Fig. 4d, the inhibitory activity of the compound on NDM-1 was affected by addition of the metals, implying that **1c** inhibits NDM-1 by removing the Zn (II) ions at active sites of the enzyme.

To further study the inhibition mechanism of thiosemicarbazone **1c** against NDM-1, dose-dependent, dialysis, Zn(II) supplement, and Zn(II) content determination experiments were performed. In the dose-dependent experiments, the concentration of meropenem is  $40\ \mu\text{M}$ , concentrations of **1c** are in the range of  $0\text{--}1.0\ \mu\text{M}$ . The concentration of Zn(II) ions in the deionized water used in the dialysis experiments was determined by ICP-MS to be  $<0.001\ \text{nM}$ . As shown in Fig. 5a, the increase of **1c** concentration resulted in the decrease of residual activity of NDM-1, when **1c** concentration is up to  $1.0\ \mu\text{M}$ , the residual activity is less than 5%, revealing that the thiosemicarbazone is a dose-dependent inhibitor of NDM-1. For the dialysis experiments, NDM-1 and **1c** ( $10\ \mu\text{M}$ ) were incubated for 1 h in advance, the processed samples ( $2\ \text{mL}$ ) were put into a  $10\ \text{kDa}$  cut-off dialysis bag and dialyzed with deionized water for 24 h, and the residual activities of NDM-1 were determined. The result (Fig. 5b) shows that the activity of NDM-1 does not change after dialysis. Afterward, the NDM-1 sample after dialysis was incubated with  $\text{ZnCl}_2$  ( $1\text{--}100\ \mu\text{M}$ ) for 30 min, and the residual activity of NDM-1 was

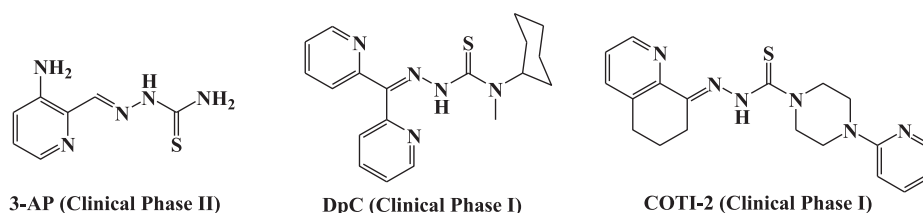


Fig. 1. Structures of thiosemicarbazones.

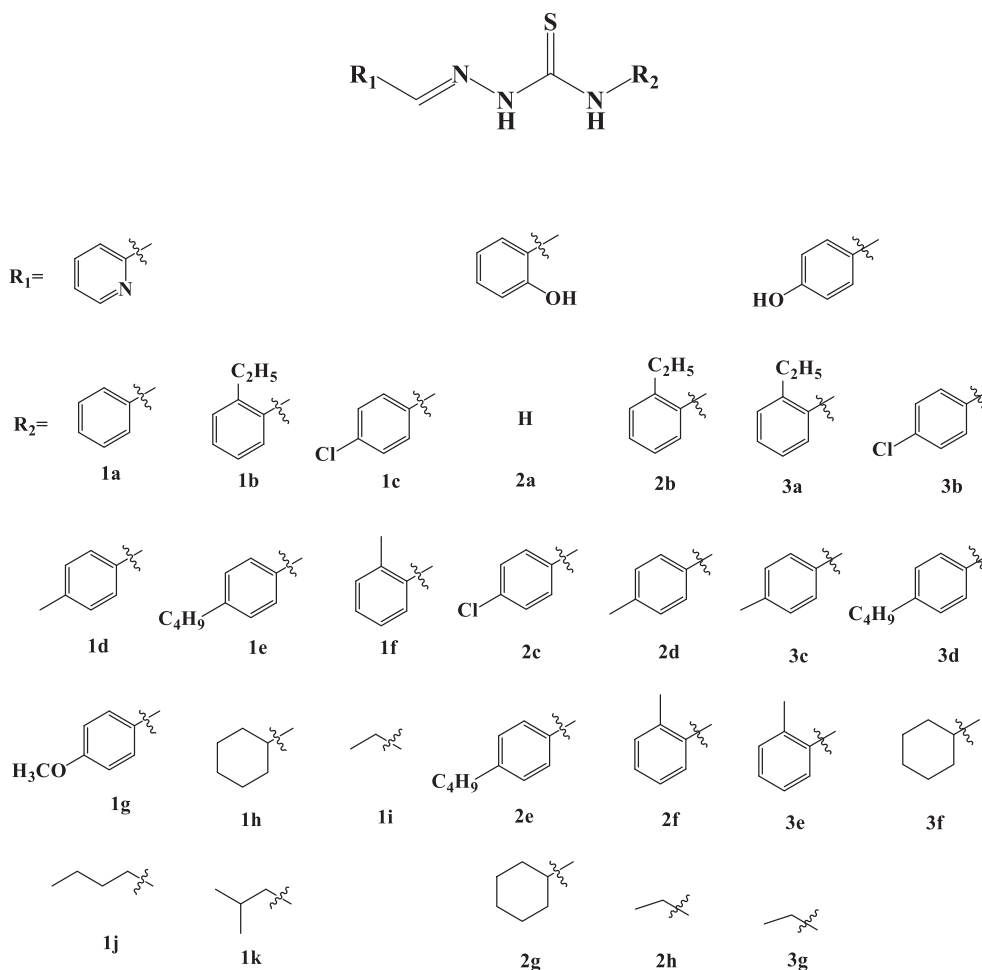
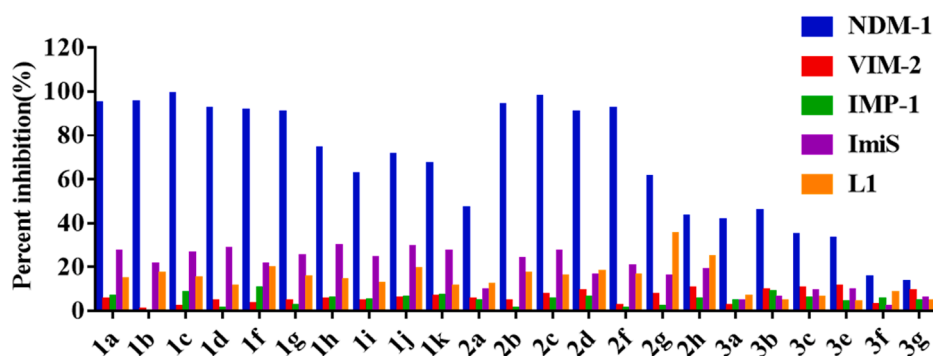


Fig. 2. Structures of synthetic thiosemicarbazones.

Fig. 3. Percent inhibition of thiosemicarbazones (5  $\mu$ M) on M $\beta$ Ls NDM-1, VIM-2, IMP-1, and L1 using meropenem (40  $\mu$ M) as substrate.

assayed. As shown in Fig. 5c, the concentration of Zn(II) increased, the activity of NDM-1 was restored, confirming that the thiosemicarbazone inhibits NDM-1 through metal chelating.

Furthermore, the dialyzed NDM-1 sample was acidized with concentrated nitric acid, and the Zn(II) content in protein was determined by inductively coupled mass spectrometry (ICP-MS). The concentrations of **1c** are in the range of 0–20  $\mu$ M. The results (Fig. 5d) revealed that NDM-1 was inactivated by **1c** and lose 1.2 equivalents of Zn(II) compared with the control group, suggesting that **1c** chelated out the Zn(II) in the active site of NDM-1, therefore exhibited inhibitory activity. Meanwhile, the percent inhibition of **1c**, **2c**, **3b** and EDTA against four M $\beta$ Ls was determined. As shown in Fig. 5e, unlike EDTA,

thiosemicarbazones specifically inhibit NDM-1.

### 2.3. Inhibition assay of NDM-1 by ITC

The thermodynamic inhibition of **1c** on NDM was investigated by isothermal titration calorimetry (ITC) on MicroCal-ITC200 in single injection mode at 25  $^{\circ}$ C [38]. The concentrations of NDM-1 and meropenem were 0.1 and 500  $\mu$ M, respectively. NDM-1 and different concentrations of **1c** (1, 2.5, 5, and 10  $\mu$ M) were incubated for 1 h in advance. A single 38  $\mu$ L of meropenem were titrated into the NDM-1-containing sample cell (210  $\mu$ L). ITC monitored inhibition progress of meropenem hydrolysis with NDM-1 by **1c** is shown in Fig. 6. Also,

**Table 1**Inhibitory activity (IC<sub>50</sub>, μM) of thiosemicarbazone derivatives against Mβl NDM-1.

| Compd.  | IC <sub>50</sub> | Compd.   | IC <sub>50</sub> |
|---|------------------|--|------------------|
| R <sub>1</sub> = 2-pyridine R <sub>2</sub> = aromatic |                  | R <sub>1</sub> = 2-pyridine R <sub>2</sub> = aliphatic |                  |
| 1a  | 0.063            | 1h   | 1.53             |
| 1b  | 0.51             | 1i   | 5.42             |
| 1c  | 0.038            | 1j   | 2.48             |
| 1d  | 0.11             | 1k   | 3.56             |
| 1e  | NA               |  |                  |
| 1f  | 0.57             |  |                  |
| 1g  | 0.27             |  |                  |
| R <sub>1</sub> = 2-hydroxyphenyl                      |                  |  |                  |
| 2a  | 6.98             | 2e   | NA               |
| 2b  | 0.47             | 2f   | 0.42             |
| 2c  | 0.12             | 2g   | 8.64             |
| 2d  | 0.28             | 2h   | 13.4             |
| R <sub>1</sub> = 4-hydroxyphenyl                      |                  |  |                  |
| 3a  | 17.8             | 3e   | 25.7             |
| 3b  | 15.4             | 3f   | >80              |
| 3c  | 19.8             | 3g   | >80              |
| 3d  | NA               |  |                  |

<sup>a</sup>NDM-1 and the thiosemicarbazones (0–80 μM) were preincubated for 1 h. NA: data is not available.

overlayed heat flow curves of meropenem (50 μM) hydrolysis by NDM-1 (25 nM) in the absence and presence of **1c** with different concentrations (0, 6.25, 25, 200, and 500 nM) are shown in Fig. S1. It can be observed that with the increase of the thiosemicarbazone concentration, the thermopower (dq/dt) and the total heat (Q) released (Fig. 6, inset) decreased gradually, confirming that **1c** is a dose-dependent inhibitor of NDM-1, similar to earlier reported the thermodynamic inhibition of eblesen on NDM-1 [38].

#### 2.4. Antibacterial activity assays in vitro

The minimum inhibitory concentration (MIC) was measured to investigate the synergistic antibacterial of thiosemicarbazones **1a–1k**, **2a–2h**, and **3a–3g** combined with meropenem against *E. coli*-NDM-1 [39]. The *E. coli* BL21 (DE3) cells with and without NDM-1 were used for assays of the inhibitors (16 μg/mL). The enhancement of the antibacterial effect of meropenem on *E. coli* NDM-1 can be observed in Table 2A

when it is used combined with most thiosemicarbazones (except **3a**, **3f**, and **3g**), resulted in a 2–512-fold reduction in MICs, while the inhibitors with aromatic R<sub>2</sub> groups exhibited stronger synergistic antibacterial ability than that with aliphatic R<sub>2</sub> substrates, and **1c** had the strongest ability, reflecting the consistency of the ability to inhibit NDM-1.

Moreover, the synergistic antibacterial effect of thiosemicarbazone and meropenem (MER) against eight clinical pathogenic bacteria producing NDM-1 were assayed. The collected MIC data (Table 2B) shown that **1c** exhibited strong activity on all clinical bacteria tested, resulting in a 512-, 16–128-, 16-, and 2-fold reduction in MIC of meropenem against *E. coli*, EC01-EC10, *K. pneumonia*, and *P. aeruginosa*, respectively, confirming that activity response of the antibiotic is due to the inhibition of thiosemicarbazone to NDM-1 in living bacterial cells.

To verify the synergistic antibacterial effect of thiosemicarbazone and meropenem (MER) against *E. coli*-NDM-1, the zone of inhibition experiment was studied. As shown in Fig. 7, the inhibitory zones used in combination of **1c** and meropenem are much larger than that of meropenem alone, and also, increasing the amount of inhibitor could improve the bacteriostatic ability of meropenem.

Given the excellent inhibitory activity of **1c**, we investigated the synergistic effect of **1c** and meropenem at different concentrations on *E. coli*-NDM-1. The concentrations of MER and **1c** are in the range of 0–256 and 0–64 μg/mL, respectively. It can be observed in Fig. 8a that **1c** alone had no inhibition for the growth of bacteria at a concentration up to 64 μg/mL, but significantly reduced the MIC of MER in combination with the antibiotic, indicating that thiosemicarbazone restored the antibacterial activity of MER by inhibiting NDM-1.

Next, **1c** was chosen to conduct the dose-dependent antibacterial assay against *E. coli*-NDM-1 and clinical pathogenic bacteria EC08. It is observed in Fig. 8b that with the increase of inhibitor concentration, the MIC values of MER decreased. When the concentration of **1c** is up to 64 μg/mL, MIC of MER against *E. coli*-NDM-1 and EC08 decreased 512 and 256-fold, respectively.

The sterilization efficiency of **1c** in combination with MER was tested by time-killing kinetics, EC08 was used for the assay, the concentration of inhibitor and MER was 16 and 32 μg/mL, respectively. It can be observed in Fig. 8c that MER alone cannot kill EC08, but MER combination with **1c** rapidly killed the bacteria as shown in Fig. 8d.

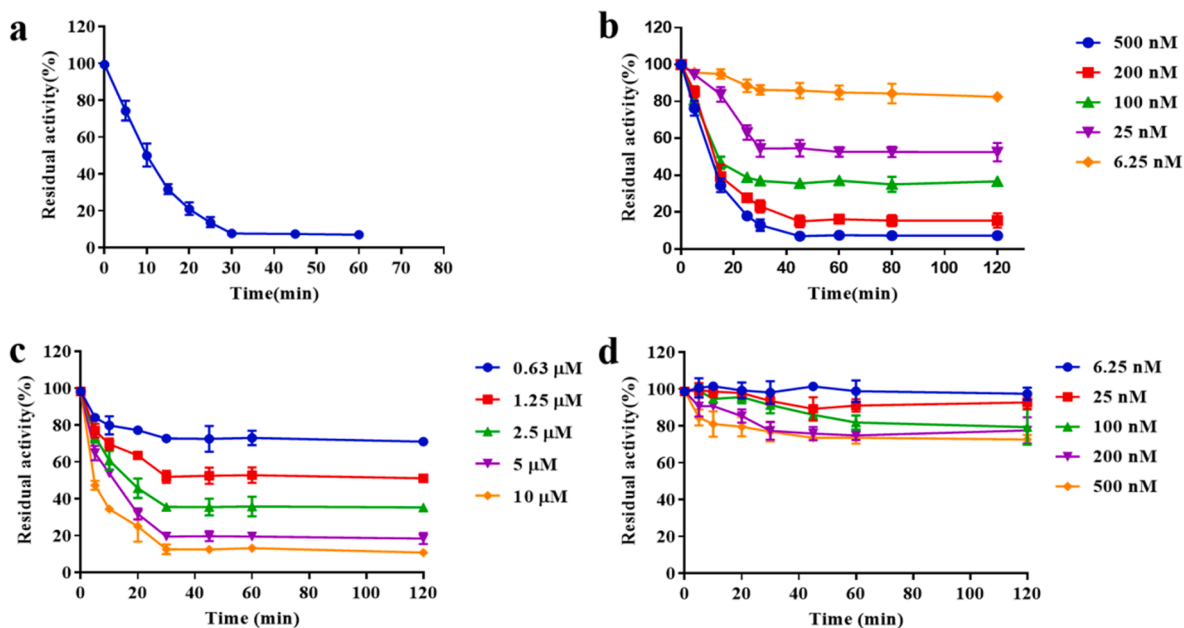


**Fig. 4.** Time- and concentration-dependent inhibition of NDM-1 by thiosemicarbazone **1c** and EDTA. Monitoring of NDM-1 inhibition by **1c** (5 μM) for 60 min (a) and by **1c** (6.25–500 nM) for 120 min (b), and by EDTA (0.63–10 μM) for 120 min (c), and by **1c** (6.25–500 nM) in the presence of Zn(II) ions for 120 min (d).

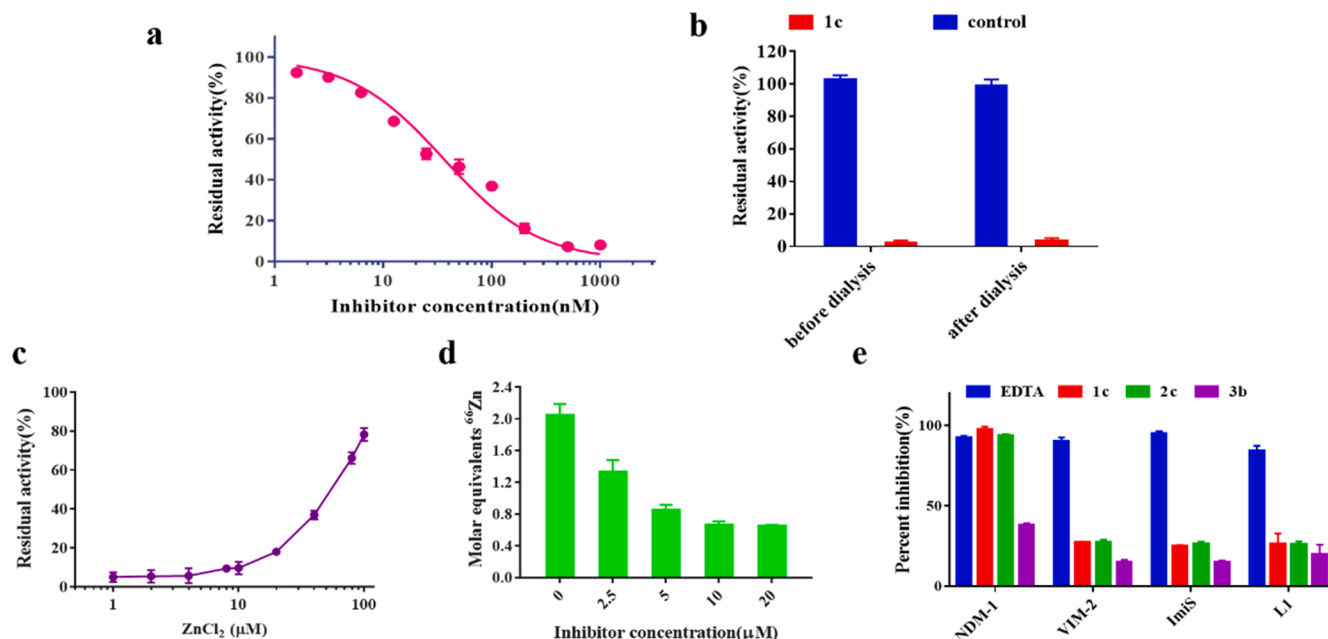


**Fig. 5.** The inhibitory mode of thiosemicarbazone **1c** on NDM-1. a, the  $IC_{50}$  curve of **1c** inhibits NDM-1; b, dialysis experiments proved that the activity of NDM-1 did not change after dialysis; c, addition of excess  $ZnCl_2$  restores activity of NDM-1 after inactivation; d, depletion of Zn(II) in NDM-1 was confirmed by ICP-MS; e, percent inhibitions of EDTA, **1c**, **2c** and **3b** (10  $\mu M$ ) on M $\beta$ Ls.

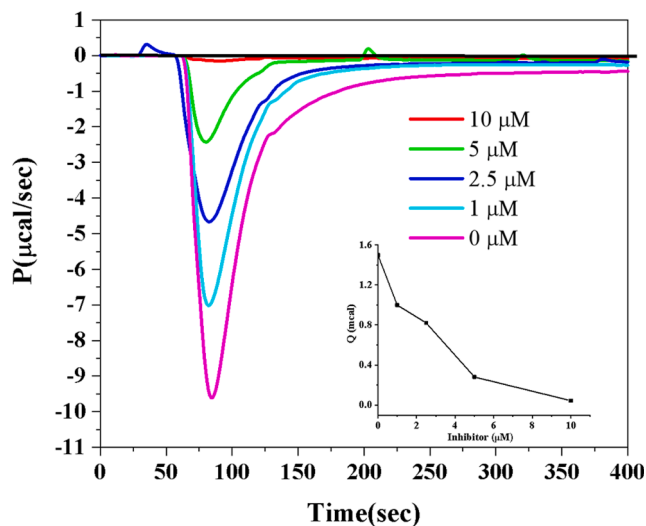


**Fig. 6.** Overlaid heat flow curves of meropenem (500  $\mu M$ ) hydrolysis by NDM-1 (0.1  $\mu M$ ) in the absence and presence of thiosemicarbazone **1c** at different concentrations (0, 1, 2.5, 5, and 10  $\mu M$ ).

### 2.5. Metal suppression experiments

To identify the effect of Zn(II) ions on thiosemicarbazone inhibitory activity, we performed the metal suppression experiments. We assayed bacterial growth of *E. coli* cells harboring NDM-1 following treatment with EDTA or **1c** in the presence of Zn(II) ions. As shown in Fig. 9, when Zn(II) ions (240  $\mu M$ ), meropenem (MER) (80  $\mu M$ ), the inhibitors (240  $\mu M$ ) EDTA or **1c** were used alone, a fluctuation of 85–92% of the bacterial growth rates was obtained. By contrast, when MER was used in combination with EDTA or **1c**, the bacterial growth rate is less than 20%. While when Zn(II) ions were pre-cultured with the combination of EDTA or **1c**, 83–85% of the bacterial growth rates were obtained. These data indicate that EDTA or **1c** used alone did not affect the growth of bacteria, while the combination of these inhibitors with MER inhibited it, at

the same time, the inhibitory activity of these compounds against NDM-1 was affected by Zn(II) ions.

### 2.6. Cytotoxicity assay

The potential toxicity of enzyme inhibitors is a principal problem for clinical medical applications. The thiosemicarbazones **1c**, **2c**, and **3b** with different working concentrations (3.13, 6.25, 12.5, 25, 50, and 100  $\mu M$ ) were subjected to a cytotoxicity assay with mouse fibroblast cells (L929) with previously reported method [39]. As shown in Fig. 10, more than 60% of the cells tested maintained viability in the presence of the inhibitors at a concentration of up to 50  $\mu M$ , suggesting that these thiosemicarbazones have certain cytotoxicity.

### 2.7. Antibacterial activity assays in vivo

The antibacterial activity of thiosemicarbazone **1c** in combination with MER *in vivo* against clinical pathogenic bacteria EC08, a mice infection model was established according to the previous method [40]. In short, Kunming mice were infected intraperitoneally with a sublethal dose of EC08. After 2 h, mice were injected intraperitoneally with a single dose of the drug. The effects of monotherapy and combination treatment of **1c** and MER on bacterial load in the liver and spleen were determined. Fig. 11 showed that monotherapy of **1c** did not affect bacterial growth compared with the control, and MER alone slightly limited bacterial growth *in vivo*. But the combination therapy of **1c** and meropenem reduced the bacterial load in the liver and spleen of mice. Antibacterial activity assays *in vivo* indicated thiosemicarbazone can cooperate with meropenem to fight the clinical challenge of carbapenem-resistant pathogens harboring NDM-1 (such as EC08).

## 3. Conclusions

Twenty-six thiosemicarbazones were synthesized and characterized by  $^1H$  and  $^{13}C$  NMR and HRMS. The biochemical evaluation revealed that all compounds (except **1e**, **2e** and **3d**) strongly inhibit NDM-1, with an  $IC_{50}$  value in the range of 0.038–5.42, 0.12–13.4, and 15.4–34.7  $\mu M$  for the 2-pyridine, 2-hydroxyphenyl, and 4-hydroxyphenyl substituted

**Table 2**

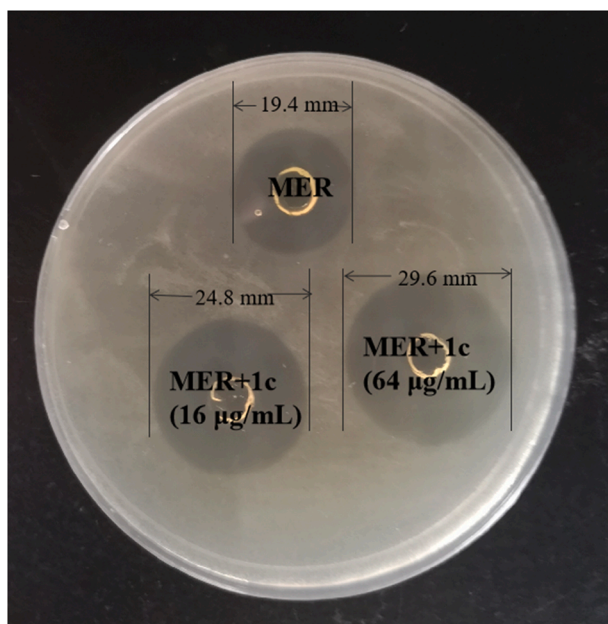
MIC of meropenem combined with thiosemicarbazones (16  $\mu\text{g}/\text{mL}$ ) against *E. coli*-NDM-1<sup>a</sup> (A), and meropenem against clinical strains harboring NDM-1, *E. coli*, *K. pneumonia*, *P. Aeruginosa*, and ECs in the presence of thiosemicarbazone **1c** (16  $\mu\text{g}/\text{mL}$ ) (B).

| A         |                       |           |                       |           |                       |
|-----------|-----------------------|-----------|-----------------------|-----------|-----------------------|
| Compd.    | <i>E. coli</i> -NDM-1 | Compd.    | <i>E. coli</i> -NDM-1 | Compd.    | <i>E. coli</i> -NDM-1 |
| MER       | 128                   | <b>1i</b> | 64                    | <b>2g</b> | 64                    |
| <b>1a</b> | 4                     | <b>1j</b> | 64                    | <b>2h</b> | 64                    |
| <b>1b</b> | 8                     | <b>1k</b> | 64                    | <b>3a</b> | 128                   |
| <b>1c</b> | 0.25                  | <b>2a</b> | 64                    | <b>3b</b> | 64                    |
| <b>1d</b> | 4                     | <b>2b</b> | 32                    | <b>3c</b> | 16                    |
| <b>1e</b> | 8                     | <b>2c</b> | 4                     | <b>3d</b> | 64                    |
| <b>1f</b> | 8                     | <b>2d</b> | 16                    | <b>3e</b> | 32                    |
| <b>1g</b> | 8                     | <b>2e</b> | 16                    | <b>3f</b> | 128                   |
| <b>1h</b> | 16                    | <b>2f</b> | 32                    | <b>3g</b> | 128                   |

| B              |                |      |      |      |      |      |                     |                      |
|----------------|----------------|------|------|------|------|------|---------------------|----------------------|
| Compd.         | <i>E. coli</i> | EC01 | EC04 | EC07 | EC08 | EC10 | <i>K. pneumonia</i> | <i>P. aeruginosa</i> |
| MER            | 128            | 64   | 32   | 64   | 128  | 128  | 32                  | 64                   |
| MER+ <b>1c</b> | 0.25           | 4    | 2    | 1    | 1    | 2    | 2                   | 32                   |

<sup>a</sup> The MIC of meropenem alone against *E. coli* cells without NDM-1 is 0.125  $\mu\text{g}/\text{mL}$ .



**Fig. 7.** The resistance of *E. coli* producing NDM-1 were tested by inhibition zone experiments. Meropenem (MER): MH with meropenem only; MER + **1c** (16  $\mu\text{g}/\text{mL}$ ), and MER + **1c** (64  $\mu\text{g}/\text{mL}$ ). MER concentration used was 32  $\mu\text{g}/\text{mL}$ .

molecules, respectively, **1c** is the most potent inhibitor ( $\text{IC}_{50} = 0.038 \mu\text{M}$ ), and **3f** and **3g** had  $\text{IC}_{50}$  values more than 80  $\mu\text{M}$ . Analysis of the  $\text{IC}_{50}$  data reveals a structure–activity relationship, which is that the  $\text{R}_1$  substituents 2-pyridine and 2-hydroxybenzene significantly improved inhibitory activities of the inhibitors against NDM-1 as compared to the same substituents at 4-position, and the aromatic  $\text{R}_2$  substituents make the inhibitors have better activities than the aliphatic substituents. MIC tests demonstrated that the thiosemicarbazones restored a 2–512-fold antimicrobial activity of meropenem on *E. coli* expressing NDM-1, specifically **1c** restored 16–256-, 16-, 2-fold activity of the antibiotic on clinical isolates ECs, *K. pneumonia* and *P. aeruginosa* harboring NDM-1, respectively. Mice experiments showed that **1c** had synergistic antibacterial efficacy with meropenem, reduced the load of clinical bacteria EC08 in the spleen and liver after a single intraperitoneal dose. These studies indicated that the thiosemicarbazone is an effective scaffold for the development of NDM-1 inhibitors.

## 4. Experimental

### 4.1. Materials

<sup>1</sup>H and <sup>13</sup>C NMR spectra were recorded on a Japan Electronics 400 MHz MRI. Chemical shifts are given in parts per million (ppm) on the delta scale. The peak patterns are recorded as singlet (s), doublet (d), triplet (t), quartet (q), doublet doublet (dd), and mul-triplet (m). The spectra were recorded with TMS as internal standard. Coupling constants ( $J$ ) were reported in Hertz (Hz). Mass spectra were obtained on a micro TOF-Q (BRUKER) mass spectrometer. Determination of enzyme inhibitory activity of compounds on Agilent 8453 UV–Vis spectrometer.

### 4.2. Synthesis of thiosemicarbazones (**1a-1k**, **2a-2h** and **3a-3g**) [41–43]

Primary amine (5 mmol) was added to 15 mL of the mixed solution of ethanol and water (1:1). Then,  $\text{CS}_2$  (5 eq) and triethylamine (1 eq) were added to the solution, and the solution was stirred at room temperature overnight. Iodine elemental (dissolved in acetonitrile, 1 eq) was slowly added to the mixture and stirred until yellow precipitated out. After further reaction for 30 min, the organic solvent was concentrated and extracted with *n*-hexane. The organic phase was washed with saturated brine and dried over anhydrous sodium sulfate. Concentrating on the organic phase, and 10 mL of isopropanol was added. In an ice bath, hydrazine hydrate was slowly added to isothiocyanate-containing isopropanol and stirred for 10 min until the precipitate was completely precipitated. The precipitate was filtered and dried under vacuum.

The dried thiosemicarbazone and the corresponding aldehyde (1 eq) were dissolved into the mixture of water and ethanol (1:1). Pyrrole (0.1 eq) was added to the solution as a catalyst. The solution was refluxed at 100 °C for 3–4 h, then cooled to room temperature, and allowed to stand overnight until crystals precipitated. The precipitated crystals were filtered and dried to give the product (**1a-1k**, **2a-2h**, and **3a-3g**).

#### 4.2.1. (*E*)-4-phenyl-1-(pyridin-2-ylmethylene)thiosemicarbazide (**1a**)

White solid, yield 74%. <sup>1</sup>H NMR (400 MHz, DMSO)  $\delta$ : 11.99 (s, 1H), 10.21 (s, 1H), 8.55 (d,  $J = 4.8$  Hz, 1H), 8.41 (d,  $J = 8.0$  Hz, 1H), 8.17 (s, 1H), 7.81 (td,  $J = 7.9, 1.5$  Hz, 1H), 7.52 (d,  $J = 8.1$  Hz, 2H), 7.42–7.30 (m, 3H), 7.19 (t,  $J = 7.4$  Hz, 1H). <sup>13</sup>C NMR (101 MHz, DMSO)  $\delta$ : 176.50, 153.24, 149.42, 143.15, 139.03, 136.56, 128.19, 126.17, 125.62, 124.32, 120.70. HRMS (ESI)  $m/z$ : 279.0689 (Calcd. for  $[\text{M} + \text{Na}]^+$  279.0674).

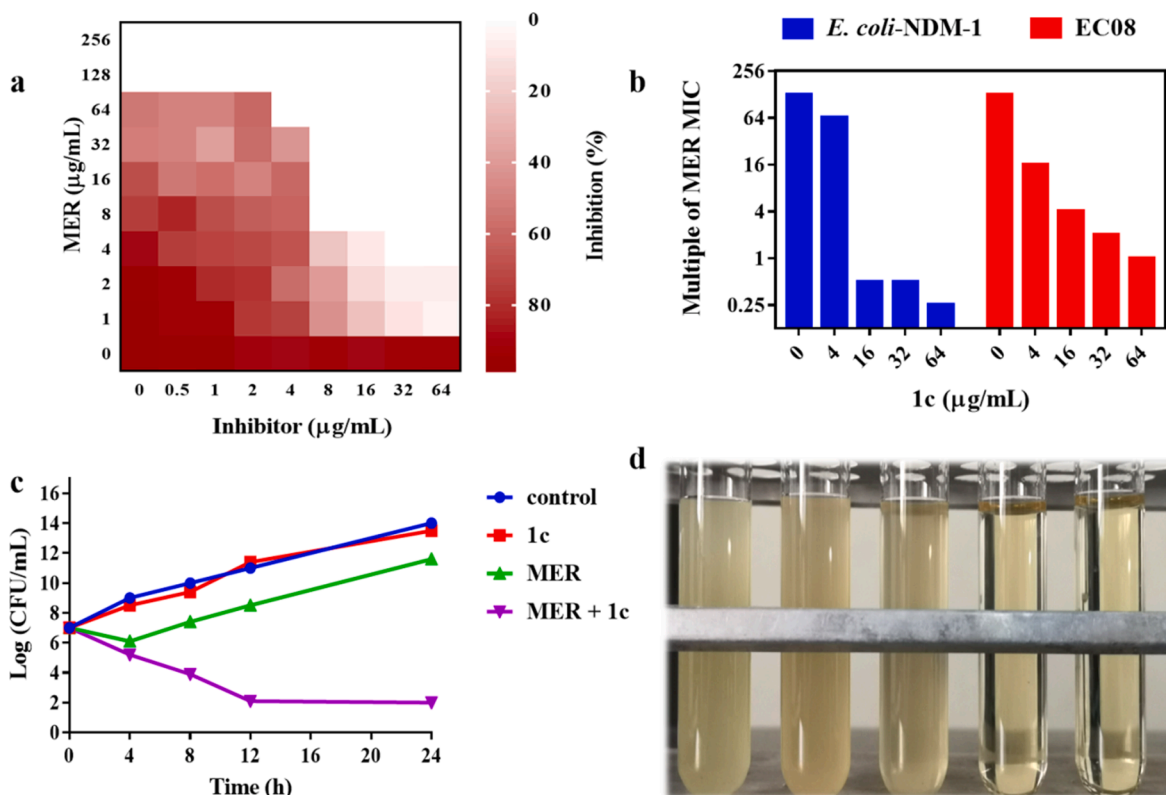


**Fig. 8.** a, Representative heat plots of microdilution checkerboard assay for the combination of Meropenem (MER); b, dose-dependent antibacterial assays of the thiosemicarbazone (0–64 (64 μg/mL) against EC08 and *E. coli*-NDM-1; c, time kill kinetics curves for MER (32 μg/mL) and 1c (64 μg/mL) monotherapy and combination therapy against EC08 during a 24 h incubation; d, the picture of the bacterial growth after 24 h.

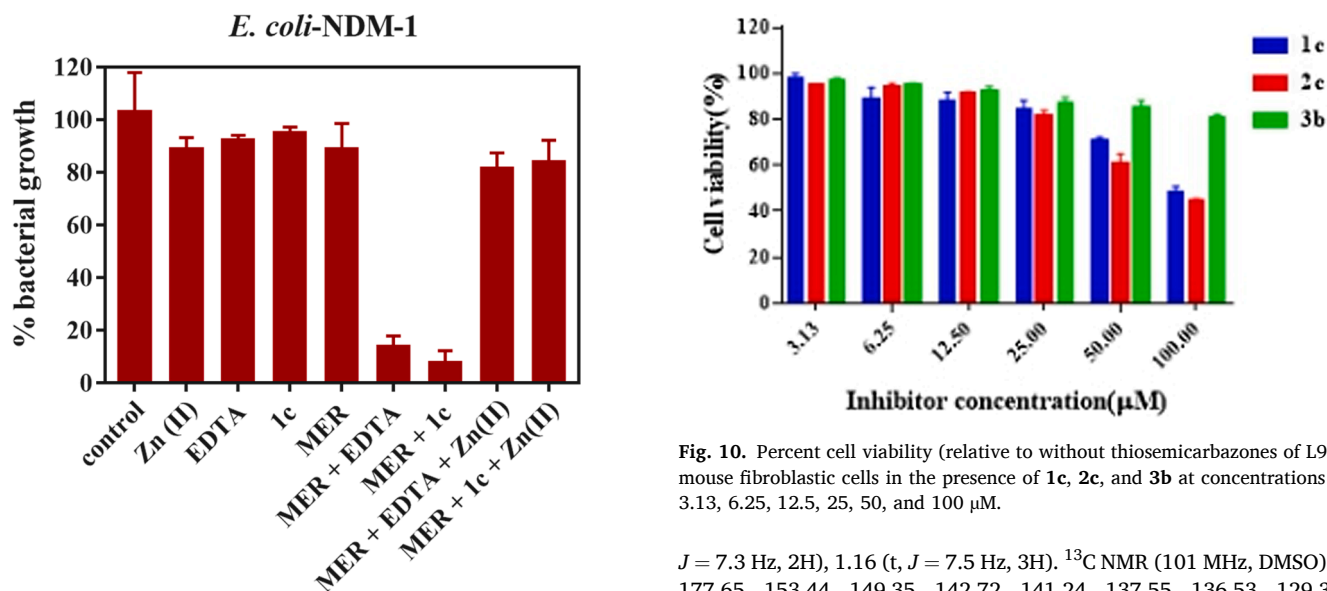


**Fig. 9.** Growth of *E. coli* cells-NDM-1 in the presence of MER (80 μM, as control), inhibitors (240 μM) EDTA or thiosemicarbazone 1c, combination of MER with the inhibitors, and the combination with additional Zn(II) ions. Zn(II) ions were from ZnCl<sub>2</sub> (240 μM).

#### 4.2.2. (*E*)-4-(2-ethylphenyl)-1-(pyridin-2-ylmethylene)thiosemicarbazide (1b)

White solid, yield 76%. <sup>1</sup>H NMR (400 MHz, DMSO) δ: 12.00 (s, 1H), 10.13 (s, 1H), 8.67–8.53 (m, 1H), 8.44 (d, *J* = 7.5 Hz, 1H), 8.20 (s, 1H), 7.82 (t, *J* = 7.5 Hz, 1H), 7.43–7.35 (m, 1H), 7.34–7.21 (m, 4H), 2.61 (d,

**Fig. 10.** Percent cell viability (relative to without thiosemicarbazones) of L929 mouse fibroblastic cells in the presence of 1c, 2c, and 3b at concentrations of 3.13, 6.25, 12.5, 25, 50, and 100 μM.

*J* = 7.3 Hz, 2H), 1.16 (t, *J* = 7.5 Hz, 3H). <sup>13</sup>C NMR (101 MHz, DMSO) δ: 177.65, 153.44, 149.35, 142.72, 141.24, 137.55, 136.53, 129.35, 128.38, 127.20, 125.97, 124.19, 120.55, 24.16, 14.28. HRMS (ESI) *m/z*: 307.1021 (Calcd. for [M + Na]<sup>+</sup> 307.0988).

#### 4.2.3. (*E*)-4-(4-chlorophenyl)-1-(pyridin-2-ylmethylene)thiosemicarbazide (1c)

White solid, yield 84%. <sup>1</sup>H NMR (400 MHz, DMSO) δ 12.11 (s, 1H), 10.29 (s, 1H), 8.59 (d, *J* = 4.7 Hz, 1H), 8.43 (d, *J* = 8.0 Hz, 1H), 8.21 (s, 1H), 7.85 (t, *J* = 7.7 Hz, 1H), 7.61 (d, *J* = 8.7 Hz, 2H), 7.48–7.36 (m, 3H). <sup>13</sup>C NMR (101 MHz, DMSO) δ: 176.52, 153.15, 149.46, 143.48, 138.02, 136.59, 129.64, 128.10, 124.41, 120.75. HRMS (ESI) *m/z*:

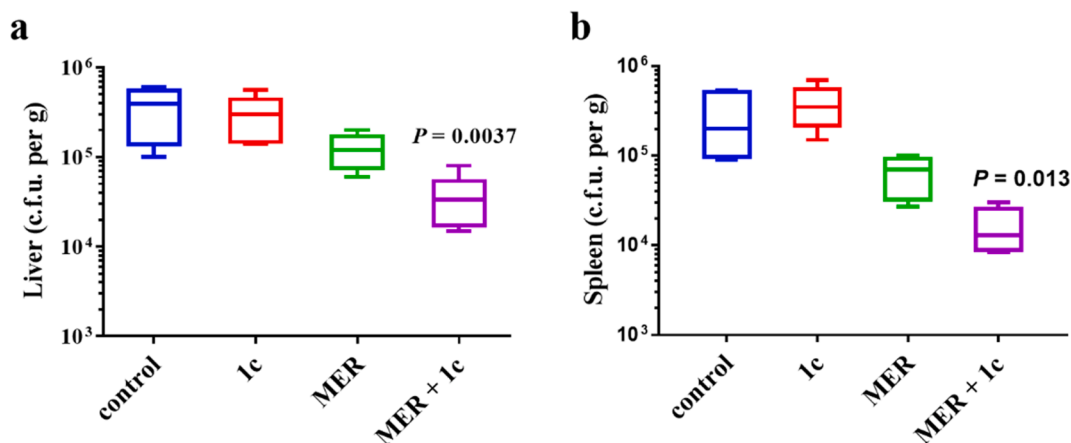


**Fig. 11.** The antibacterial activity of thiosemicarbazone **1c** in combination with MER against EC08 *in vivo*. Groups of mice infected by EC08 were treated with a single dose of meropenem (10 mg/kg), **1c** (2 mg/kg), a combination of MER (10 mg/kg) and **1c** (2 mg/kg), and EC08 (as control) by intraperitoneal injection. Bacterial load in the liver (a) and spleen (b) was determined by selective plating.

313.0291 (Calcd. for  $[M + Na]^+$  313.0285).

#### 4.2.4. (*E*)-1-(pyridin-2-ylmethylene)-4-*p*-tolylthiosemicarbazide (**1d**)

White needle crystal, yield 82%.  $^1\text{H}$  NMR (400 MHz, DMSO)  $\delta$ : 11.98 (s, 1H), 10.18 (s, 1H), 8.58 (d,  $J = 4.5$  Hz, 1H), 8.44 (d,  $J = 8.1$  Hz, 1H), 8.19 (s, 1H), 7.84 (t,  $J = 8.5$  Hz, 1H), 7.45–7.35 (m, 3H), 7.18 (d,  $J = 8.2$  Hz, 2H), 2.32 (s, 3H).  $^{13}\text{C}$  NMR (101 MHz, DMSO)  $\delta$ : 176.55, 153.28, 149.40, 143.00, 136.54, 134.80, 128.66, 126.09, 124.28, 120.68, 20.69. HRMS (ESI)  $m/z$ : 293.0850 (Calcd. for  $[M + Na]^+$  293.0831).

#### 4.2.5. (*E*)-4-(4-butylphenyl)-1-(pyridin-2-ylmethylene)thiosemicarbazide (**1e**)

White needle crystal, yield 78%.  $^1\text{H}$  NMR (400 MHz, DMSO)  $\delta$ : 11.99 (s, 1H), 10.19 (s, 1H), 8.58 (d,  $J = 6.0$  Hz, 1H), 8.44 (d,  $J = 7.9$  Hz, 1H), 8.19 (s, 1H), 7.84 (t,  $J = 8.5$  Hz, 1H), 7.45–7.30 (m, 3H), 7.19 (d,  $J = 8.3$  Hz, 2H), 2.67–2.53 (m, 2H), 1.56 (p,  $J = 7.5$  Hz, 2H), 1.32 (dt,  $J = 14.8$ , 7.3 Hz, 2H), 0.90 (t,  $J = 7.4$  Hz, 3H).  $^{13}\text{C}$  NMR (101 MHz, DMSO)  $\delta$ : 176.47, 153.30, 149.40, 142.99, 139.75, 136.55, 128.00, 126.09, 124.29, 120.67, 34.44, 33.27, 21.80, 13.88. HRMS (ESI)  $m/z$ : 335.1327 (Calcd. for  $[M + Na]^+$  335.1301).

#### 4.2.6. (*E*)-1-(pyridin-2-ylmethylene)-4-*o*-tolylthiosemicarbazide (**1f**)

White solid, yield 88%.  $^1\text{H}$  NMR (400 MHz, DMSO)  $\delta$ : 10.09 (s, 1H), 8.54 (d,  $J = 4.4$  Hz, 1H), 8.39 (d,  $J = 8.0$  Hz, 1H), 8.15 (s, 1H), 7.79 (t,  $J = 8.4$  Hz, 1H), 7.40–7.28 (m, 1H), 7.28–7.14 (m, 4H), 2.20 (s, 3H).  $^{13}\text{C}$  NMR (101 MHz, DMSO)  $\delta$ : 177.27, 153.41, 149.37, 142.75, 138.06, 136.55, 135.68, 130.17, 128.90, 126.95, 126.05, 124.21, 120.57, 17.85. HRMS (ESI)  $m/z$ : 293.0852 (Calcd. for  $[M + Na]^+$  293.0831).

#### 4.2.7. (*E*)-4-(4-methoxyphenyl)-1-(pyridin-2-ylmethylene)thiosemicarbazide (**1g**)

White solid, yield 75%.  $^1\text{H}$  NMR (400 MHz, DMSO)  $\delta$ : 11.96 (s, 1H), 10.16 (s, 1H), 8.58 (d,  $J = 4.4$  Hz, 1H), 8.44 (d,  $J = 8.0$  Hz, 1H), 8.18 (s, 1H), 7.83 (t,  $J = 8.3$  Hz, 1H), 7.38 (t,  $J = 7.8$  Hz, 3H), 6.94 (d,  $J = 8.9$  Hz, 2H), 3.77 (s, 3H).  $^{13}\text{C}$  NMR (101 MHz, DMSO)  $\delta$ : 176.86, 157.18, 153.34, 149.41, 142.91, 136.56, 131.92, 127.83, 124.28, 120.68, 113.41, 55.34. HRMS (ESI)  $m/z$ : 309.0794 (Calcd. for  $[M + Na]^+$  309.0781).

#### 4.2.8. (*E*)-4-cyclohexyl-1-(pyridin-2-ylmethylene)thiosemicarbazide (**1h**)

White solid, yield 88%.  $^1\text{H}$  NMR (400 MHz, DMSO)  $\delta$ : 11.64 (s, 1H), 8.56 (d,  $J = 4.7$  Hz, 1H), 8.26 (d,  $J = 8.0$  Hz, 1H), 8.18 (d,  $J = 8.5$  Hz, 1H), 8.10 (s, 1H), 7.84 (t,  $J = 7.7$  Hz, 1H), 7.40–7.33 (m, 1H), 4.21 (dt,  $J = 12.1$ , 8.6, 3.8 Hz, 1H), 1.87 (d,  $J = 10.0$  Hz, 2H), 1.73 (d,  $J = 12.7$  Hz, 2H), 1.61 (d,  $J = 12.2$  Hz, 1H), 1.45 (q,  $J = 1.8$ , 10.8 Hz, 2H), 1.28

(q,  $J = 12.6$  Hz, 2H), 1.12 (q,  $J = 12.4$  Hz, 1H).  $^{13}\text{C}$  NMR (101 MHz, DMSO)  $\delta$ : 176.00, 153.30, 149.44, 142.47, 136.58, 124.19, 120.45, 52.98, 31.84, 25.09. HRMS (ESI)  $m/z$ : 285.1169 (Calcd. for  $[M + Na]^+$  285.1144).

#### 4.2.9. (*E*)-4-ethyl-1-(pyridin-2-ylmethylene)thiosemicarbazide (**1i**)

White needle crystal, yield 92%.  $^1\text{H}$  NMR (400 MHz, DMSO)  $\delta$ : 11.64 (s, 1H), 8.70 (t,  $J = 5.8$  Hz, 1H), 8.55 (d,  $J = 4.8$  Hz, 1H), 8.25 (d,  $J = 8.0$  Hz, 1H), 8.09 (s, 1H), 7.83 (t,  $J = 7.7$  Hz, 1H), 7.43–7.26 (m, 1H), 3.61 (p,  $J = 7.0$  Hz, 2H), 1.16 (t,  $J = 7.1$  Hz, 3H).  $^{13}\text{C}$  NMR (101 MHz, DMSO)  $\delta$ : 176.99, 153.44, 149.40, 142.12, 136.51, 124.09, 120.23, 38.47, 14.60. HRMS (ESI)  $m/z$ : 231.0700 (Calcd. for  $[M + Na]^+$  231.0675).

#### 4.2.10. (*E*)-4-butyl-1-(pyridin-2-ylmethylene)thiosemicarbazide (**1j**)

White solid, yield 65%.  $^1\text{H}$  NMR (400 MHz, DMSO)  $\delta$ : 11.62 (s, 1H), 8.66 (t,  $J = 5.6$  Hz, 1H), 8.56 (d,  $J = 4.5$  Hz, 1H), 8.26 (d,  $J = 7.9$  Hz, 1H), 8.09 (s, 1H), 7.84 (t,  $J = 7.7$  Hz, 1H), 7.40–7.32 (m, 1H), 3.57 (q,  $J = 6.6$  Hz, 2H), 1.58 (p,  $J = 7.5$  Hz, 2H), 1.32 (h,  $J = 7.4$  Hz, 2H), 0.91 (t,  $J = 7.3$  Hz, 3H).  $^{13}\text{C}$  NMR (101 MHz, DMSO)  $\delta$ : 177.18, 153.44, 149.39, 142.11, 136.52, 124.09, 120.23, 43.37, 31.04, 19.67, 13.89. HRMS (ESI)  $m/z$ : 237.1167 (Calcd. for  $[M + H]^+$  237.1168).

#### 4.2.11. (*E*)-4-isobutyl-1-(pyridin-2-ylmethylene)thiosemicarbazide (**1k**)

White solid, yield 56%.  $^1\text{H}$  NMR (400 MHz, DMSO)  $\delta$ : 11.64 (s, 1H), 8.66 (t,  $J = 5.9$  Hz, 1H), 8.56 (d,  $J = 4.9$  Hz, 1H), 8.26 (d,  $J = 8.1$  Hz, 1H), 8.10 (s, 1H), 7.84 (td,  $J = 7.8$ , 1.6 Hz, 1H), 7.37 (ddd,  $J = 7.3$ , 4.9, 0.9 Hz, 1H), 3.44–3.38 (m, 2H), 2.04 (dq,  $J = 13.6$ , 6.8 Hz, 1H), 0.89 (d,  $J = 6.8$  Hz, 7H).  $^{13}\text{C}$  NMR (101 MHz, DMSO)  $\delta$ : 177.55, 153.42, 149.41, 142.18, 136.56, 124.11, 120.24, 50.95, 27.89, 20.19. HRMS (ESI)  $m/z$ : 237.1190 (Calcd. for  $[M + H]^+$  237.1168).

#### 4.2.12. (*E*)-1-(2-hydroxybenzylidene)thiosemicarbazide (**2a**)

White solid, yield 95%.  $^1\text{H}$  NMR (400 MHz, DMSO)  $\delta$ : 11.38 (s, 1H), 9.87 (s, 1H), 8.37 (s, 1H), 8.11 (s, 1H), 7.91 (d,  $J = 6.3$  Hz, 2H), 7.30–7.13 (m, 1H), 6.94–6.71 (m, 2H).  $^{13}\text{C}$  NMR (101 MHz, DMSO)  $\delta$ : 177.75, 156.53, 139.78, 131.25, 126.88, 120.46, 119.43, 116.17. HRMS (ESI)  $m/z$ : 196.0515 (Calcd. for  $[M + H]^+$  196.0539).

#### 4.2.13. (*E*)-1-(2-hydroxybenzylidene)-4-(2-ethylphenyl)thiosemicarbazide (**2b**)

Light yellow solid, yield 72%.  $^1\text{H}$  NMR (400 MHz, DMSO)  $\delta$ : 11.72 (s, 1H), 9.89 (s, 2H), 8.48 (s, 1H), 8.06 (d,  $J = 7.3$  Hz, 1H), 7.25 (ddd,  $J = 24.1$ , 9.7, 5.0 Hz, 5H), 6.88 (d,  $J = 8.1$  Hz, 1H), 6.82 (t,  $J = 7.5$  Hz, 1H), 2.60 (q,  $J = 7.5$  Hz, 2H), 1.15 (t,  $J = 7.6$  Hz, 3H).  $^{13}\text{C}$  NMR (101 MHz, DMSO)  $\delta$ : 176.99, 156.59, 140.95, 137.69, 131.25, 129.17, 128.33,

126.91, 125.87, 119.33, 116.12, 24.19, 14.28. HRMS (ESI)  $m/z$ : 300.1157 (Calcd. for  $[M + H]^+$  300.1165).

4.2.14. (*E*)-1-(2-hydroxybenzylidene)-4-(4-chlorophenyl)thiosemicarbazide (2c)

White solid, yield 69%.  $^1\text{H}$  NMR (400 MHz, DMSO)  $\delta$ : 11.86 (s, 1H), 10.04 (d,  $J = 45.0$  Hz, 2H), 8.51 (t,  $J = 9.0$  Hz, 1H), 8.19–7.96 (m, 1H), 7.63 (d,  $J = 7.5$  Hz, 2H), 7.41 (d,  $J = 8.3$  Hz, 2H), 7.34–7.13 (m, 1H), 6.87 (dt,  $J = 15.0, 7.7$  Hz, 2H).  $^{13}\text{C}$  NMR (101 MHz, DMSO)  $\delta$ : 175.77, 156.75, 140.50, 138.24, 131.52, 129.24, 127.99, 127.41, 127.16, 120.29, 119.32, 116.15. HRMS (ESI)  $m/z$ : 328.0256 (Calcd. for  $[M + \text{Na}]^+$  328.0282).

4.2.15. (*E*)-1-(2-hydroxybenzylidene)-4-*p*-tolylthiosemicarbazide (2d)

White solid, yield 74%.  $^1\text{H}$  NMR (400 MHz, DMSO)  $\delta$ : 11.72 (s, 1H), 9.98 (s, 2H), 8.50 (d,  $J = 6.5$  Hz, 1H), 8.09 (s, 1H), 7.43 (d,  $J = 8.0$  Hz, 2H), 7.30–7.05 (m, 3H), 6.86 (dt,  $J = 14.4, 7.6$  Hz, 2H), 2.30 (s, 3H).  $^{13}\text{C}$  NMR (101 MHz, DMSO)  $\delta$ : 175.87, 156.65, 140.05, 136.67, 134.42, 131.36, 128.59, 127.17, 125.76, 120.38, 119.31, 116.12, 20.69. HRMS (ESI)  $m/z$ : 308.0808 (Calcd. for  $[M + \text{Na}]^+$  308.0828).

4.2.16. (*E*)-1-(2-hydroxybenzylidene)-4-(4-butylphenyl)thiosemicarbazide (2e)

White solid, yield 82%.  $^1\text{H}$  NMR (400 MHz, DMSO)  $\delta$ : 11.73 (s, 1H), 9.98 (s, 2H), 8.50 (s, 1H), 8.24–8.03 (m, 1H), 7.46 (d,  $J = 8.1$  Hz, 2H), 7.30–7.05 (m, 3H), 7.05–6.71 (m, 2H), 2.58 (d,  $J = 7.1$  Hz, 2H), 1.55 (d,  $J = 6.8$  Hz, 2H), 1.44–1.17 (m, 2H), 0.91 (q,  $J = 8.2, 7.1$  Hz, 3H).  $^{13}\text{C}$  NMR (101 MHz, DMSO)  $\delta$ : 175.81, 156.67, 140.02, 139.36, 136.85, 131.35, 127.92, 127.17, 125.69, 120.38, 119.31, 116.12, 34.47, 33.31, 21.84, 13.90. HRMS (ESI)  $m/z$ : 328.1465 (Calcd. for  $[M + H]^+$  328.1478).

4.2.17. (*E*)-1-(2-hydroxybenzylidene)-4-*o*-tolylthiosemicarbazide (2f)

White solid, yield 76%.  $^1\text{H}$  NMR (400 MHz, DMSO)  $\delta$ : 11.73 (s, 1H), 9.90 (s, 2H), 8.48 (s, 1H), 8.08 (d,  $J = 6.8$  Hz, 1H), 7.37–7.09 (m, 5H), 6.94–6.71 (m, 2H), 2.24 (s, 3H).  $^{13}\text{C}$  NMR (101 MHz, DMSO)  $\delta$ : 161.22, 141.18, 122.82, 120.00, 115.85, 114.69, 113.29, 111.71, 111.25, 110.53, 105.05, 103.91, 100.70, 2.50. HRMS (ESI)  $m/z$ : 308.0827 (Calcd. for  $[M + \text{Na}]^+$  308.0828).

4.2.18. (*E*)-1-(2-hydroxybenzylidene)-4-cyclohexylthiosemicarbazide (2g)

White solid, yield 85%.  $^1\text{H}$  NMR (400 MHz, DMSO)  $\delta$ : 11.35 (s, 1H), 9.92 (s, 1H), 8.38 (s, 1H), 7.92 (dd,  $J = 19.8, 8.0$  Hz, 2H), 7.22 (t,  $J = 7.6$  Hz, 1H), 6.85 (dd,  $J = 16.9, 8.1$  Hz, 2H), 4.31–4.03 (m, 1H), 1.91–1.10 (m, 10H).  $^{13}\text{C}$  NMR (101 MHz, DMSO)  $\delta$ : 175.64, 156.50, 139.39, 131.14, 126.74, 120.45, 119.30, 116.12, 52.63, 31.94, 25.02. HRMS (ESI)  $m/z$ : 300.1142 (Calcd. for  $[M + \text{Na}]^+$  300.1141).

4.2.19. (*E*)-1-(2-hydroxybenzylidene)-4-ethylthiosemicarbazide (2h)

White solid, yield 79%.  $^1\text{H}$  NMR (400 MHz, DMSO)  $\delta$ : 11.35 (s, 1H), 9.88 (s, 1H), 8.41 (d,  $J = 30.7$  Hz, 2H), 7.93 (d,  $J = 7.5$  Hz, 1H), 7.20 (d,  $J = 7.1$  Hz, 1H), 7.02–6.68 (m, 2H), 3.66–3.45 (m, 2H), 1.14 (dd,  $J = 8.7, 5.2$  Hz, 3H).  $^{13}\text{C}$  NMR (101 MHz, DMSO)  $\delta$ : 176.58, 156.44, 139.17, 131.09, 126.75, 120.55, 119.30, 116.13, 38.38, 14.76. HRMS (ESI)  $m/z$ : 224.0852 (Calcd. for  $[M + H]^+$  224.0852).

4.2.20. (*E*)-1-(4-hydroxybenzylidene)-4-(2-ethylphenyl)thiosemicarbazide (3a)

White solid, yield 82%.  $^1\text{H}$  NMR (400 MHz, DMSO)  $\delta$ : 11.62 (s, 1H), 9.86 (d,  $J = 23.1$  Hz, 2H), 8.06 (s, 1H), 7.72 (d,  $J = 8.6$  Hz, 2H), 7.39–7.11 (m, 4H), 6.80 (d,  $J = 8.6$  Hz, 2H), 2.61 (q,  $J = 7.5$  Hz, 2H), 1.15 (t,  $J = 7.6$  Hz, 3H).  $^{13}\text{C}$  NMR (101 MHz, DMSO)  $\delta$ : 176.77, 159.44, 142.92, 140.95, 137.72, 129.40, 128.31, 126.89, 125.86, 125.25, 115.63, 24.20, 14.29. HRMS (ESI)  $m/z$ : 322.0976 (Calcd. for  $[M + \text{Na}]^+$  322.0985).

4.2.21. (*E*)-1-(4-hydroxybenzylidene)-4-(4-chlorophenyl)thiosemicarbazide (3b)

White solid, yield 74%.  $^1\text{H}$  NMR (400 MHz, DMSO)  $\delta$ : 11.75 (s, 1H), 10.03 (s, 1H), 9.94 (s, 1H), 8.08 (s, 1H), 7.73 (d,  $J = 8.6$  Hz, 2H), 7.64 (d,  $J = 8.8$  Hz, 2H), 7.41 (d,  $J = 8.8$  Hz, 2H), 6.82 (d,  $J = 8.7$  Hz, 2H).  $^{13}\text{C}$  NMR (101 MHz, DMSO)  $\delta$ : 175.46, 159.65, 143.76, 138.24, 129.63, 129.20, 127.98, 127.35, 124.98, 115.66. HRMS (ESI)  $m/z$ : 328.0258 (Calcd. for  $[M + \text{Na}]^+$  328.0282).

4.2.22. (*E*)-1-(4-hydroxybenzylidene)-4-*p*-tolylthiosemicarbazide (3c)

White solid, yield 69%.  $^1\text{H}$  NMR (400 MHz, DMSO)  $\delta$ : 11.61 (s, 1H), 9.92 (s, 2H), 8.07 (s, 1H), 7.73 (d,  $J = 8.5$  Hz, 2H), 7.44 (d,  $J = 8.2$  Hz, 2H), 7.16 (d,  $J = 8.1$  Hz, 2H), 6.81 (d,  $J = 8.5$  Hz, 2H), 2.30 (s, 3H).  $^{13}\text{C}$  NMR (101 MHz, DMSO)  $\delta$ : 175.59, 159.54, 143.28, 136.68, 134.39, 129.54, 128.59, 125.73, 125.11, 115.65, 20.71. HRMS (ESI)  $m/z$ : 308.0815 (Calcd. for  $[M + \text{Na}]^+$  308.0828).

4.2.23. (*E*)-1-(4-hydroxybenzylidene)-4-(4-butylphenyl)thiosemicarbazide (3d)

White solid, yield 82%.  $^1\text{H}$  NMR (400 MHz, DMSO)  $\delta$ : 11.60 (s, 1H), 9.91 (s, 2H), 8.06 (s, 1H), 7.72 (d,  $J = 8.6$  Hz, 2H), 7.46 (d,  $J = 8.2$  Hz, 2H), 7.17 (d,  $J = 8.2$  Hz, 2H), 6.80 (d,  $J = 8.6$  Hz, 2H), 2.58 (t,  $J = 7.6$  Hz, 2H), 1.57 (p,  $J = 8.0, 7.6$  Hz, 2H), 1.31 (dt,  $J = 14.3, 7.3$  Hz, 2H), 0.91 (d,  $J = 14.6$  Hz, 3H).  $^{13}\text{C}$  NMR (101 MHz, DMSO)  $\delta$ : 175.48, 159.51, 143.22, 139.30, 136.84, 129.50, 127.88, 125.67, 125.08, 115.60, 34.43, 33.29, 21.81, 13.88. HRMS (ESI)  $m/z$ : 328.1476 (Calcd. for  $[M + H]^+$  328.1478).

4.2.24. (*E*)-1-(4-hydroxybenzylidene)-4-*o*-tolylthiosemicarbazide (3e)

White solid, yield 76%.  $^1\text{H}$  NMR (400 MHz, DMSO)  $\delta$ : 11.62 (s, 1H), 9.89 (s, 1H), 9.84 (s, 1H), 8.06 (s, 1H), 7.72 (d,  $J = 8.7$  Hz, 2H), 7.34–7.29 (m, 1H), 7.27 (dd,  $J = 6.6, 2.3$  Hz, 1H), 7.25–7.16 (m, 2H), 6.80 (d,  $J = 8.7$  Hz, 2H), 2.24 (s, 3H).  $^{13}\text{C}$  NMR (101 MHz, DMSO)  $\delta$ : 176.42, 159.45, 142.93, 138.26, 135.42, 130.11, 129.43, 128.73, 126.63, 125.94, 125.24, 115.63, 17.95. HRMS (ESI)  $m/z$ : 308.0822 (Calcd. for  $[M + \text{Na}]^+$  308.0828).

4.2.25. (*E*)-1-(4-hydroxybenzylidene)-4-cyclohexylthiosemicarbazide (3f)

White solid, yield 85%.  $^1\text{H}$  NMR (400 MHz, DMSO)  $\delta$ : 11.23 (s, 1H), 9.88 (s, 1H), 7.97 (s, 1H), 7.86 (d,  $J = 8.6$  Hz, 1H), 7.60 (d,  $J = 8.6$  Hz, 2H), 6.80 (d,  $J = 8.6$  Hz, 2H), 4.18 (ddt,  $J = 15.3, 11.0, 4.7$  Hz, 1H), 1.92–1.82 (m, 2H), 1.77–1.66 (m, 2H), 1.60 (d,  $J = 12.4$  Hz, 1H), 1.42 (qd,  $J = 12.1, 2.8$  Hz, 2H), 1.28 (q,  $J = 12.4$  Hz, 2H), 1.13 (q,  $J = 12.3$  Hz, 1H).  $^{13}\text{C}$  NMR (101 MHz, DMSO)  $\delta$ : 175.40, 159.35, 142.64, 129.16, 125.13, 115.64, 52.55, 32.01, 25.26, 25.03. HRMS (ESI)  $m/z$ : 278.1340 (Calcd. for  $[M + H]^+$  278.1322).

4.2.26. (*E*)-1-(4-hydroxybenzylidene)-4-ethylthiosemicarbazide (3g)

White solid, yield 82%.  $^1\text{H}$  NMR (400 MHz, DMSO)  $\delta$ : 11.23 (s, 1H), 9.86 (s, 1H), 8.37 (d,  $J = 5.7$  Hz, 1H), 7.96 (s, 1H), 7.62 (d,  $J = 8.6$  Hz, 2H), 6.79 (d,  $J = 8.6$  Hz, 2H), 3.58 (p,  $J = 6.9$  Hz, 2H), 1.14 (t,  $J = 7.1$  Hz, 3H).  $^{13}\text{C}$  NMR (101 MHz, DMSO)  $\delta$ : 176.41, 159.29, 142.32, 129.08, 125.31, 115.63, 38.29, 14.82. HRMS (ESI)  $m/z$ : 224.0855 (Calcd. for  $[M + H]^+$  224.0852).

4.3. Determination of  $\text{IC}_{50}$  and percent inhibition

NDM-1, VIM-2, IMP-1, ImiS, and L1 were over-expressed and purified. The concentration of the substrate (meropenem) was 40  $\mu\text{M}$ . 10 mM thiosemicarbazones (**1a-1k**, **2a-2h**, and **3a-3g**) were dissolved in DMSO and diluted to final concentration at a range of 0–80  $\mu\text{M}$  (the content of DMSO after dilution is less than 5%) to determine the  $\text{IC}_{50}$  value. The percent inhibition rates were determined at an inhibitor concentration of 5  $\mu\text{M}$ . Measuring antibiotic hydrolysis rates on the Agilent UV8453 spectrometer and determine three times in parallel.

#### 4.4. Isothermal titration calorimetry (ITC) assays

The thermodynamic inhibition of **1c** against NDM-1 was determined by the ITC experiment on a Malvern MicroCal iTC 200 instruments. NDM-1 and different concentrations of **1c** (1, 2.5, 5, and 10  $\mu\text{M}$ ) were incubated for 1 h in advance. A single 38  $\mu\text{L}$  of meropenem were titrated into the NDM-1-containing sample cell (210  $\mu\text{L}$ ). The final concentration of NDM-1 is 100 nM. Heat flow was recorded as a function of time and the experimental data were processed by MicroCal Analysis Launcher Origin 7 software.

#### 4.5. Determination of MIC

The minimum inhibitory concentration (MIC) of the compounds or meropenem alone and a combination of meropenem and thiosemicarbazones were determined using the broth micro-dilution method and the Clinical and Laboratory Standards Institute (CLSI) method. The solutions of *E. coli* containing NDM-1 and clinical isolates containing NDM-1 (EC01-EC08, *K. pneumoniae*, and *P. aeruginosa*) were cultivated to  $\text{OD}_{600} = 0.4\text{--}0.6$  and were diluted 84-fold. The above clinical isolates are from the General Hospital of the Southern War Zone of the Chinese people's Liberation Army and the Health Science Center at Xi'an Jiaotong University (Xian, China). Thiosemicarbazones were dissolved in DMSO and diluted to a concentration of 64  $\mu\text{g}/\text{mL}$  (DMSO content is less than 5%). Antibiotic solutions were prepared as 0.25–128  $\mu\text{g}/\text{mL}$  stock solutions (dilute in multiples of 2). 50  $\mu\text{L}$  inhibitor (final concentration, 16  $\mu\text{g}/\text{mL}$ ), 50  $\mu\text{L}$  antibiotics with different concentrations (0.25–128  $\mu\text{g}/\text{mL}$ ) and 100  $\mu\text{L}$  bacterial solution was mixed and incubated at 37  $^{\circ}\text{C}$  for 16–24 h. All experiments were measured in parallel three times.

#### 4.6. Time-dependent kill assay

To further explore the synergistic antibacterial effect of **1c** and meropenem against clinical bacteria EC08, a time-dependent kill experiment was studied. In short, bacteria were incubated and diluted to the concentration of  $\sim 10^7$  CFU/mL. EC08 was treated with **1c** (16  $\mu\text{g}/\text{mL}$ ), meropenem (32  $\mu\text{g}/\text{mL}$ ) and a combination of meropenem (32  $\mu\text{g}/\text{mL}$ ) and **1c** (16  $\mu\text{g}/\text{mL}$ ). At different time intervals (0–24 h), aliquots of bacterial suspensions were taken to determine the number of bacterial colonies by agar plates.

#### 4.7. Determination of Zn(II) content

The concentrations of Zn(II) ions in the buffer used in the kinetic experiments and in the deionized water used in the dialysis experiments, and the ability of **1c** to chelate Zn(II) from purified NDM-1 were analyzed by ICP-MS. The purified NDM-1 was diluted to a concentration of 20  $\mu\text{M}$ . Different concentrations of thiosemicarbazone **1c** (2.5, 5, 10, and 20  $\mu\text{M}$ ) and NDM-1 were incubated at 4  $^{\circ}\text{C}$  for 1 h. The processed samples (2 mL) were put into a 10 kDa cut-off dialysis bag and dialyzed with deionized water for 24 h. Deionized water was changed every 6 h during dialysis. Next, samples were added 5% concentrated nitric acid and heated for 10 min. Samples were diluted to the measured concentration (NDM-1 at a final concentration of 4  $\mu\text{M}$ ) by adding deionized water. Zn(II) content of processed samples was analyzed by ICP-MS. The samples tested were transferred by nebulization into the ICP MS spectrometer. Quantitative analysis was performed in triplicate for each sample with 60 sweeps per reading using the peak-hopping mode with a 50 ms/AMU dwell time for each element. Instrument settings were: rf power (1600 W), integration time (35 s), collision gas ( $^{40}\text{Ar}$ ), RPQ voltage (25 V) and sample flow rate (4 r.p.m.). Isotope abundance was determined by integrating peak areas using the NexION software program, and the data was represented graphically using Microsoft Excel. A calibration curve with four standards and a correlation coefficient of greater than 0.999 was generated using Zn reference solutions.

#### 4.8. Metal suppression experiments

In metal suppression experiments, bacterial growth of *E. coli* cells harboring NDM-1 following treatment with EDTA or **1c** in the presence of Zn(II) ions was assayed. The concentration of MER was 80  $\mu\text{M}$ , and concentration of Zn(II) ions and inhibitors was 240  $\mu\text{M}$ . *E. coli* cells with  $\text{OD}_{600}$  of 0.4–0.6 were diluted 84-fold, 3 mL inhibitor (or 3 mL combination of inhibitor and  $\text{ZnCl}_2$ ), 3 mL MER and 6 mL bacteria were mixed and incubated at 37  $^{\circ}\text{C}$  for 16 h. The  $\text{OD}_{600}$  values of *E. coli* cells were measured on Agilent UV8453 spectrometer. The  $\text{OD}_{600}$  value of the control group is considered to be 100% bacterial growth rate. The bacterial growth rate of other groups was calculated according to the measured  $\text{OD}_{600}$  values. The average results were plotted as the mean  $\pm$  SD of the three experiments.

#### 4.9. Cytotoxicity assay

A cytotoxicity of inhibitors **1c**, **2c** and **3b** to mouse fibro-blast cells (L929) was assayed. The cells with a density of  $1.0 \times 10^4$  cells/well in 100  $\mu\text{L}$  of culture medium were seeded into 96-well plates and maintained for 24 h. Then solutions of inhibitors **1c**, **2c** and **3b** with work concentrations (3.13, 6.25, 12.5, 25, 50, and 100  $\mu\text{M}$ ) were added to 96-well plates, respectively, and incubated for another 48 h. Six wells containing only cells suspended in a mixture of 99  $\mu\text{L}$  of complete medium and 1  $\mu\text{L}$  of DMSO were used as the control for investigating cell-viability. Three wells containing only the complete medium were used as the blank control. Following that, the medium was removed, and 100  $\mu\text{L}$  of fresh culture medium and 10  $\mu\text{L}$  of CCK8 were added to each well. After incubation for 4 h, the 96-well plates were then vigorously shaken to solubilize the formed product and the absorbance at a wavelength of 490 nm was read on a Microplate Reader and analyzed. All experiments were conducted in triplicate.

#### 4.10. Mice experiments

The mice experiment was approved by the Animal Medicine Committee of Xi'an Jiaotong University, and all experimental steps complied with the Guidelines for Care and Use of Laboratory Animals of Xi'an Jiaotong University. Animals were given the sterile ultrapure water and standard commercial diet quantitatively. The mice were randomly divided into four groups, and male and female were cultured separately, with six mice in each group. The bacteria were cultured to an  $\text{OD}_{600}$  value of 0.8, and 150  $\mu\text{L}$  of bacterial solution was injected into the abdominal cavity of mice. After infection for 2 h, the mice infected group were conducted intraperitoneal treatment with MHB, thiosemicarbazone **1c** (2 mg/kg), and meropenem (10 mg/kg), a combination of meropenem (10 mg/kg) and **1c** (2 mg/kg). The weight of liver and spleen of each mice were kept the same and added with 1 mL of sterile PBS to homogenate for 3–5 min. The slurries were dilute serially, placed 10  $\mu\text{L}$  on LB-agar plates and counted the number of colonies.

#### Declaration of Competing Interest

The authors declare that they have no known competing financial interests or personal relationships that could have appeared to influence the work reported in this paper.

#### Acknowledgements

This work was supported by the grants (22077100 and 2019KW-068 to K.W.Y.) from National Natural Science Foundation of China and Shaanxi Province International Cooperation Project and grant (201710010013 to Z.H.J.) from the Science and Technology Program of Guangzhou, China.

## Appendix A. Supplementary material

Supplementary data to this article can be found online at <https://doi.org/10.1016/j.bioorg.2020.104576>.

## References

- [1] S.M. Drawz, R.A. Bonomo, Three decades of beta-lactamase inhibitors, *Clin. Microbiol. Rev.* 23 (2010) 160–201.
- [2] G. Cornaglia, H. Giamarellou, G.M. Rossolini, Metallo- $\beta$ -lactamases: a last frontier for  $\beta$ -lactams? *Lancet Infect. Dis.* 11 (2011) 381–393.
- [3] M.W. Crowder, J. Spencer, A.J. Vila, Metallo-beta-lactamases: novel weaponry for antibiotic resistance in bacteria, *Acc. Chem. Res.* 39 (2006) 721–728.
- [4] K. Bush, G.A. Jacoby, Updated functional classification of beta-lactamases, *Antimicrob. Agents Chemother.* 54 (2010) 969–976.
- [5] Z.X. Hu, G. Periyannan, B. Bennett, M.W. Crowder, Role of the Zn-1 and Zn-2 sites in Metallo-beta-lactamase L1, *J. Am. Chem. Soc.* 130 (2008) 14207–14216.
- [6] G. Garau, I. Garcia-Saez, C. Bebrone, C. Anne, P. Mercuri, M. Galleni, J.M. Frere, O. Dideberg, Update of the standard numbering scheme for class B beta-lactamases, *Antimicrob. Agents Chemother.* 48 (2004) 2347–2349.
- [7] D.Y. Wang, M.I. Abboud, M.S. Markoulides, J. Brem, C.J. Schofield, The road to avibactam: the first clinically useful non-beta-lactam working somewhat like a beta-lactam, *Future Med. Chem.* 8 (2016) 1063–1084.
- [8] J.L. Liscio, M.V. Mahoney, E.B. Hirsch, Ceftolozane/tazobactam and ceftazidime/avibactam: two novel beta-lactam/beta-lactamase inhibitor combination agents for the treatment of resistant Gram-negative bacterial infections, *Int. J. Antimicrob. Agents* 46 (2015) 266–271.
- [9] D.M. Shlaes, New  $\beta$ -lactam- $\beta$ -lactamase inhibitor combinations in clinical development, *Ann. N. Y. Acad. Sci.* 1277 (2013) 105–114.
- [10] S. Liu, L. Jing, Z.J. Yu, C.Y. Wu, Y.X. Zheng, E. Zhang, Q. Chen, Y.M. Yu, L. Guo, Y. Wu, G.B. Li, ((S)-3-Mercapto-2-methylpropanoimido)acetic acid derivatives as metallo-beta-lactamase inhibitors: Synthesis, kinetic and crystallographic studies, *Eur. J. Med. Chem.* 145 (2018) 649–660.
- [11] P. Hinchliffe, M.M. Gonzalez, M.F. Mojica, J.M. Gonzalez, V. Castillo, C. Saiz, M. Kosmopoulou, C.L. Tooke, L.I. Llarrull, G. Mahler, R.A. Bonomo, A.J. Vila, J. Spencer, Cross-class metallo-beta-lactamase inhibition by bisthiazolidines reveals multiple binding modes, *Proc. Natl. Acad. Sci. U. S. A.* 113 (2016) E3745–E3754.
- [12] J. Brem, S.S. van Berkel, D. Zollman, S.Y. Lee, O. Gileadi, P.J. McHugh, T.R. Walsh, M.A. McDonough, C.J. Schofield, Structural basis of metallo-beta-lactamase inhibition by captopril stereoisomers, *Antimicrob. Agents Chemother.* 60 (2016) 142–150.
- [13] T. Christopheit, T.J.O. Carlsen, R. Helland, H.K.S. Leiros, Discovery of novel inhibitor scaffolds against the metallo-beta-lactamase VIM-2 by surface plasmon resonance (SPR) based fragment screening, *J. Med. Chem.* 58 (2015) 8671–8682.
- [14] A.L.Y. Chen, P.W. Thomas, A.C. Stewart, A. Bergstrom, Z.S. Cheng, C. Miller, C. R. Bethel, S.H. Marshal, C.V. Credille, C.L. Riley, R.C. Page, R.A. Bonomo, M. W. Crowder, D.L. Tierney, W. Fast, S.M. Cohen, Dipicolinic acid derivatives as inhibitors of New Delhi metallo-beta-lactamase-1, *J. Med. Chem.* 60 (2017) 7267–7283.
- [15] J.C. Chiou, S.B. Wan, K.F. Chan, P.K. So, D.D. He, E.W.C. Chan, T.H. Chan, K. Y. Wong, J. Tao, S. Chen, Ebselen as a potent covalent inhibitor of New Delhi metallo-beta-lactamase (NDM-1), *Chem. Commun.* 51 (2015) 9543–9546.
- [16] C. Chen, Y. Xiang, K.W. Yang, Y.J. Zhang, W.M. Wang, J.P. Su, Y. Ge, Y. Liu, A protein structure-guided covalent scaffold selectively targets the B1 and B2 subclass metallo-beta-lactamases, *Chem. Commun.* 54 (2018) 4802–4805.
- [17] D. Zhang, M.S. Markoulides, D. Stepanovs, A.M. Rydzik, A. El-Husseini, C. Bon, J. Kamps, K.D. Umland, P.M. Collins, S.T. Cahill, D.Y. Wang, F. von Delft, J. Brem, M.A. McDonough, C.J. Schofield, Structure activity relationship studies on rhodanines and derived enethiol inhibitors of metallo-beta-lactamases, *Bioorg. Med. Chem.* 26 (2018) 2928–2936.
- [18] Y. Xiang, C. Chen, W.M. Wang, L.W. Xu, K.W. Yang, P. Oelschlaeger, Y. He, Rhodanine as a potent scaffold for the development of broad spectrum metallo-beta-lactamase inhibitors, *ACS Med. Chem. Lett.* 9 (2018) 359–364.
- [19] J. Brem, S.S. van Berkel, W. Aik, A.M. Rydzik, M.B. Avison, I. Pettinati, K. D. Umland, A. Kawamura, J. Spencer, T.D.W. Claridge, M.A. McDonough, C. J. Schofield, Rhodanine hydrolysis leads to potent thioenolate mediated metallo-beta-lactamase inhibition, *Nat. Chem.* 6 (2014) 1084–1090.
- [20] A. Parkova, A. Lucic, A. Krajnc, J. Brem, K. Calvopina, G.W. Langley, M. A. McDonough, P. Trapencieris, C.J. Schofield, Broad spectrum beta-lactamase inhibition by a thioether substituted bicyclic boronate, *ACS Infect. Dis.* 6 (2020) 1398–1404.
- [21] O. Lomovskaya, R. Tsvikovski, K. Nelson, D. Rubio-Aparicio, D.X. Sun, M. Totrov, M.N. Dudley, Spectrum of beta-lactamase inhibition by the cyclic boronate QPX7728, an ultrabroad-spectrum beta-lactamase inhibitor of serine and metallo-beta-lactamases: enhancement of activity of multiple antibiotics against isogenic strains expressing single beta-lactamases, *Antimicrob. Agents Chemother.* 64 (2020) e00212–e220.
- [22] J. Brem, R. Cain, S. Cahill, M.A. McDonough, L.J. Clifton, J.C. Jimenez-Castellanos, M.B. Avison, J. Spencer, C.W.G. Fishwick, C.J. Schofield, Structural basis of metallo-beta-lactamase, serine-beta-lactamase and penicillin-binding protein inhibition by cyclic boronates, *Nat. Commun.* 7 (2016) 12406.
- [23] A.U. Khan, L. Maryam, R. Zarrilli, Structure, genetics and worldwide spread of New Delhi metallo-beta-lactamase (NDM): a threat to public health, *BMC Microbiol.* 17 (2017) 12.
- [24] T.R. Walsh, Emerging carbapenemases: a global perspective, *Int. J. Antimicrob. Agents* 36 (2010) S8–S14.
- [25] C.M. Gill, M.J. Lasko, T.E. Asempa, D.P. Nicolau, Evaluation of the EDTA-modified carbapenem inactivation method for detecting metallo-beta-lactamase-producing *Pseudomonas aeruginosa*, *J. Clin. Microbiol.* 58 (2020).
- [26] A.M. King, S.A. Reid-Yu, W.L. Wang, D.T. King, G. De Pascale, N.C. Strynadka, T. R. Walsh, B.K. Coombes, G.D. Wright, Aspergillomarasmine A overcomes metallo-beta-lactamase antibiotic resistance, *Nature* 510 (2014) 503–506.
- [27] A.M. Somboro, D. Tiwari, L.A. Bester, R. Parboosing, L. Chonco, H.G. Kruger, P. I. Arvidsson, T. Govender, T. Naicker, S.Y. Essack, NOTA: a potent metallo-beta-lactamase inhibitor, *J. Antimicrob. Chemother.* 70 (2015) 1594–1596.
- [28] S.B. Falconer, S.A. Reid-Yu, A.M. King, S.S. Gehrke, W.L. Wang, J.F. Britten, B. K. Coombes, G.D. Wright, E.D. Brown, Zinc chelation by a small-molecule adjuvant potentiates meropenem activity in vivo against NDM-1-producing klebsiella pneumoniae, *ACS Infect. Dis.* 1 (2015) 533–543.
- [29] C.R. Nishida, P.R.O. de Montellano, Bioactivation of antituberculosis thioamide and thiourea prodrugs by bacterial and mammalian flavin monooxygenases, *Chem.-Biol. Interact.* 192 (2011) 21–25.
- [30] B. Sarkanj, M. Molnar, M. Cacic, L. Gille, 4-Methyl-7-hydroxycoumarin antifungal and antioxidant activity enhancement by substitution with thiosemicarbazide and thiazolidinone moieties, *Food Chem.* 139 (2013) 488–495.
- [31] V.F.S. Pape, S. Toth, A. Furedi, K. Szebenyi, A. Lovrics, P. Szabo, M. Wiese, G. Szakacs, Design, synthesis and biological evaluation of thiosemicarbazones, hydrazinobenzothiazoles and arylhydrazones as anticancer agents with a potential to overcome multidrug resistance, *Eur. J. Med. Chem.* 117 (2016) 335–354.
- [32] P. Heffeter, V.F.S. Pape, E.A. Enyedy, B.K. Keppler, G. Szakacs, C.R. Kowol, Anticancer thiosemicarbazones: chemical properties, interaction with iron metabolism, and resistance development, *Antioxid. Redox Signal.* 30 (2019) 1062–1082.
- [33] K.L. Summers, A structural chemistry perspective on the antimalarial properties of thiosemicarbazone metal complexes, *Mini-Rev. Med. Chem.* 19 (2019) 569–590.
- [34] J. Murren, M. Modiano, C. Clairmont, P. Lambert, N. Savaraj, T. Doyle, M. Sznol, Phase I and pharmacokinetic study of triapine, a potent ribonucleotide reductase inhibitor, administered daily for five days in patients with advanced solid tumors, *Clin. Cancer Res.* 9 (2003) 4092–4100.
- [35] S. Attia, J. Kolesar, M.R. Mahoney, H.C. Pitot, D. Laheru, J. Heun, W. Huang, J. Eickhoff, C. Erlichman, K.D. Hoken, A phase 2 consortium (P2C) trial of 3-aminopyridine-2-carboxaldehyde thiosemicarbazone (3-AP) for advanced adenocarcinoma of the pancreas, *Invest. New Drugs* 26 (2008) 369–379.
- [36] Z.L. Guo, D.R. Richardson, D.S. Kalinowski, Z. Kovacevic, K.C. Tan-Un, G.C. F. Chan, The novel thiosemicarbazone, di-2-pyridylketone 4-cyclohexyl-4-methyl-3-thiosemicarbazone (DpC), inhibits neuroblastoma growth in vitro and in vivo via multiple mechanisms, *J. Hematol. Oncol.* 9 (2016) 16.
- [37] O.A. Chaves, M.R.D. Santos, M.C.C. de Oliveira, C.M.R. Sant'Anna, R.C. Ferreira, A. Echevarria, J.C. Netto-Ferreira, Synthesis, tyrosinase inhibition and transportation behavior of novel beta-enamino thiosemicarbazide derivatives by human serum albumin, *J. Mol. Liq.* 254 (2018) 280–290.
- [38] Y.J. Zhang, W.M. Wang, P. Oelschlaeger, C. Chen, J.E. Lei, M. Lv, K.W. Yang, Real-time monitoring of NDM-1 activity in live bacterial cells by isothermal titration calorimetry: a new approach to measure inhibition of antibiotic-resistant bacteria, *ACS Infect. Dis.* 4 (2018) 1671–1678.
- [39] Y. Liu, C. Chen, L.-Y. Sun, H. Gao, J.-B. Zhen, K.-W. Yang, meta-Substituted benzenesulfonamide: a potent scaffold for the development of metallo-beta-lactamase ImiS inhibitors, *RSC Med. Chem.* 11 (2020) 259–267.
- [40] C. Cheng, L.Y. Sun, H. Gao, P.W. Kang, J.Q. Li, J.B. Zhen, K.W. Yang, Identification of cisplatin and palladium(II) complexes as potent metallo-beta-lactamase inhibitors for targeting carbapenem-resistant enterobacteriaceae, *ACS Infect. Dis.* 6 (2020) 975–985.
- [41] P. Thanigaimalai, K.C. Lee, V.K. Sharma, E. Roh, Y. Kim, S.H. Jung, Ketone-thiosemicarbazones: structure-activity relationships for their melanogenesis inhibition, *Bioorg. Med. Chem. Lett.* 21 (2011) 3527–3530.
- [42] J. Nath, H. Ghosh, R. Yella, B.K. Patel, Molecular iodine mediated preparation of isothiocyanates from dithiocarbamic acid salts, *Eur. J. Org. Chem.* 2009 (2009) 1849–1851.
- [43] M.A. Khanfar, D. Reiner, S. Hagenow, H. Stark, Design, synthesis, and biological evaluation of novel oxadiazole- and thiazole-based histamine H3R ligands, *Bioorg. Med. Chem.* 26 (2018) 4034–4046.